The theory of attenuated total reflection by surface polaritons on corrugated semi-infinite media

M. Masale*

Physics Department, University of Botswana, Private Bag 0022, Gaborone, Botswana

Received 26 January 2001; received in revised form 25 September 2001

Abstract

The experimental techniques of attenuated total reflection and grating-coupling were originally employed separately as probes for surface polaritons. However, as far back as the mid-1970s, some value was found in actually combining them into a single tool for probing elementary surface excitations. In this article, the theory of the two methods combined into one probe for surface polaritons is presented. The main results of the calculations, here, are the first-order diffuse reflectivities, which arise due to the presence of a classical grating. For the ease of presentation, only a semi-infinite specimen is considered and the grating is thought to be deposited only on one interface. The discussion highlights the advantages the combined technique has over either of the two methods when each is employed on its own.

PACS: 78.20.Ci

Keywords: ATR; Grating-coupling; Surface polaritons

1. Introduction

The dispersion curve of surface polaritons propagating along a planar interface separating semi-infinite media runs far to the right of the light line [1]. This means that these modes are not accessible in ordinary optical experiments whereby light of any intensity is incident on a planar specimen [2]. Attenuated total reflection (ATR) has proved to be a versatile tool for probing surface excitations propagating along planar surfaces. Extensive experimental as well as theoretical considerations of this method may be found in the early exhaustive editions, for example, by Agranovich and Mills [3]. There have also been some theoretical [4], and recently, experimental as well as theoretical [5] investigations of surface polaritons in composite media using the ATR method. In these media, the frequency-dependent dielectric function used takes into account the inhomogeneity of the surface-active medium.

The other experimental technique which has been employed with success as a probe for surface excitations is grating coupling [6,7]. In the early stages of using this method, gratings were inscribed on specimen using diamond tools. As a result, the actual surface profile of roughness produced in this manner was poorly defined and as such it fitted a somewhat statistical rather than

*Tel.: +267-355-2940; fax: +267-585-097.
E-mail address: masalem@mopipi.ub.bw (M. Masale).

the purely deterministic character of a classical grating. There was also the view that a grating inscribed on a surface-active medium was a nuisance, perturbing the very mode under investigation. In the extensive investigations that followed [8], especially fuelled by potential applications of surface polaritons propagating along rough interfaces [9], a classical-grating simply played the role of a first-approximation model in the characterization of a statistically rough surface [10]. It was also a matter of interest to evaluate the extent to which surface modes were perturbed by surface roughness [11]. It was not long, however, before other techniques for producing well characterized gratings were developed, such as using holographic means on photoresist materials [12]. Following this lead, Heitmann and Raether [13] performed ATR measurements on thick Ag films on which a photoresist with a sinusoidally varying surface profile was deposited.

Now, light scattered from a classical grating, especially of small height, is much more coherent compared to that from a statistically rough surface. Further, in view of the great flexibility in sample preparation as well as fabrication techniques [14], grating coupling might as well be reconsidered as a probe for surface excitations. The desire to manipulate photons in a manner similar to the control of electrons in solids has led to a great deal of renewed interest in a number of research areas, for example, such as the localization of light and microcavity quantum electrodynamics. To this end, there have been extensive investigations in optical transmission of light through subwavelength hole arrays in metal films [15–17]. These arrays of periodic cylindrical cavities excite the plasmon mode analogous to the coupling of surface phonon polaritons via a classical grating.

In the investigations undertaken here, grating coupling is reconsidered, but, in combination with ATR in the Otto [18] configuration as a single tool for probing surface polaritons. The combined experimental technique of ATR and grating coupling potentially has substantial advantages over either of the above two methods when each is employed on its own. The major component of the analysis presented here is the calculations of the first-order diffuse reflectivities. For the ease of presentation only isotropic semi-infinite specimens are considered. Further, the grating is thought to be inscribed on only one interface, that is, either on the base of the prism or on the specimen.

2. Formalism

The ATR set-up in the Otto [18] configuration consists of a prism of (high) dielectric constant ε_1, occupying the region $z > 0$. The region, $-d \leqslant z \leqslant 0$, is usually the air-gap and the surface-active medium, occupying the half-space $z < -d$, is characterized by a frequency-dependent dielectric function $\varepsilon_3 = \varepsilon(\omega)$, of the form [1]

$$\varepsilon(\omega) = \varepsilon(\infty) + \frac{S\omega_T^2}{\omega_T^2 - \omega^2 - \imath\Gamma\omega}, \tag{1}$$

where $\varepsilon(\infty)$ is the high-frequency dielectric constant, S measures the strength of resonance, ω_T is the TO phonon frequency and Γ is the damping parameter. In simple systems such as those described by the dielectric function above, the polariton fields are simply plane waves. For perfectly planar surfaces, there is only one type of the polariton fields which are proportional to $e^{\imath(k_{1x}x-\omega t)}$. With the grating present, the situation is different as there emerge other types of the polariton fields. The profile of a classical grating, taking only the first Fourier component, is described by

$$u(x) = u_0(e^{\imath Qx} + e^{-\imath Qx}), \tag{2}$$

where u_0 is the grating amplitude and $Q = 2\pi/a_0$ is the reciprocal lattice vector of a grating of period a_0. The new types of waves that emerge are proportional to $e^{\imath[(k_{1x}\pm Q)x-\omega t]}$. These are identified as the first-order fields characterized by propagation in the $q_{1x}^{\pm} = k_{1x} \pm Q$ tangential components of the wave vector. It turns out; however, that in first-order perturbation theory (such as here) the two types of the first-order fields couple independently to the zero-order fields. It, therefore, suffices to consider the first-order fields for propagation in only one of the two (q_{1x}^{-} or q_{1x}^{+}) wave numbers. In fact, reversing the sign of Q in the fields for

propagation in one wave number gives the fields for propagation in the other wave number. To distinguish between the zero- and first-order fields, the amplitudes of the zero-order polariton fields are denoted by normal letters, while those for the first-order fields are denoted by script letters. The polariton fields, in p-polarization; $(E_x, 0, E_z)$, in the ℓth ($\ell = 1, 2$ and 3) region are given below as follows:

The zero-order fields, which exist even in the absence of surface roughness, are

$$E_{\ell x} = \{A_\ell e^{-ia_\ell z} + B_\ell e^{ia_\ell z}\} e^{i(k_{1x}x - \omega t)} \tag{3}$$

and

$$E_{\ell z} = \frac{k_{1x}}{a_\ell}\{A_\ell e^{-ia_\ell z} - B_\ell e^{ia_\ell z}\} e^{i(k_{1x}x - \omega t)}, \tag{4}$$

where the perpendicular a_ℓ and tangential k_{1x} components of the total wave vector are, respectively, given by

$$a_\ell^2 = \pm\left(\varepsilon_\ell \frac{\omega^2}{c^2} - k_{1x}^2\right) \quad \text{and} \quad k_{1x} = \varepsilon_1 \frac{\omega^2}{c^2}\sin^2\theta \tag{5}$$

in which $c = 1/\sqrt{\varepsilon_0\mu_0}$ is the speed of light in vacuum. The angle of incidence of the incoming radiation, θ, must be greater than the prism-air critical angle, $\theta_c = \sin^{-1}(\sqrt{\varepsilon_2}/\sqrt{\varepsilon_1})$, if total internal reflection is to occur. The tangential component of the wave vector of the incident radiation is a conserved quantity which means that $k_{1x} = k_{2x} = k_{3x}$.

The first-order fields for propagation in $q_{1x} = k_{1x} - Q$, say, are

$$\mathscr{E}_{\ell x} = \{\mathscr{A}_\ell e^{-iq_\ell z} + \mathscr{B}_\ell e^{iq_\ell z}\} e^{i(q_{1x}x - \omega t)} \tag{6}$$

and

$$\mathscr{E}_{\ell z} = \frac{q_{1x}}{q_{\ell z}}\{\mathscr{A}_\ell e^{-iq_\ell z} - \mathscr{B}_\ell e^{iq_\ell z}\} e^{i(q_{1x}x - \omega t)}, \tag{7}$$

where

$$q_{\ell z}^2 = \pm\left(\varepsilon_\ell \frac{\omega^2}{c^2} - q_{1x}^2\right). \tag{8}$$

In Eqs. (5) and (8) for the perpendicular components of the wave vectors, the upper sign (+) is taken for fields in region one and the negative sign for fields in regions two and three. The polariton fields in region one propagate freely in all spatial directions. In the other regions, there is free propagation only parallel to the interface, but the fields are attenuated in the perpendicular direction, that is, away from the interface. In addition, since the fields must be bounded as $z \to -\infty$, the coefficients B_3 and $\mathscr{B}_3$ must be zero. Further, since the first-order fields originate from the surface, the coefficient $\mathscr{A}_1$ must be taken as zero. This is to say that the diffuse radiation is not a component of the incident radiation.

2.1. The modified boundary conditions

The usual boundary conditions at a planar surface now have to be modified to take into account the undulation of the surface, which is in the z-direction. The polariton fields are referred to a coordinate system which is simply a rotation of the ordinary Cartesian coordinates through an angle γ. This new coordinate system is chosen so that the tangential component of the electric field is always in the interface [19]. The tangential E_t and the normal E_n components of the electric field, respectively, are related to the x- and z-components according to

$$\begin{pmatrix} E_t \\ E_n \end{pmatrix} = \begin{pmatrix} \cos\gamma & \sin\gamma \\ -\sin\gamma & \cos\gamma \end{pmatrix}\begin{pmatrix} E_x \\ E_z \end{pmatrix}. \tag{9a}$$

For a grating of small amplitude, the components of the electric field, E_t and E_n, may be written as follows:

$$E_t = \frac{E_x + u'(x)E_z}{\sqrt{1 + u'^2(x)}}, \tag{9b}$$

$$E_n = \frac{E_z - u'(x)E_x}{\sqrt{1 + u'^2(x)}}, \tag{9c}$$

where $u'(x) = \partial u(x)/\partial x$. It may be inferred from Eqs. (9b) and (9c) that because of the undulation of the surface, the crystal imparts momentum $\pm\hbar Q$, to the incident radiation. This in turn generates the diffuse fields which are proportional to $e^{i[(k_{1x}\pm Q)x - \omega t]}$. The modified boundary conditions are then a continuity of E_t and εE_n at the interface [20], located at $z = u(x)$ or at $z = -d + u(x)$. For a grating of small height, only the leading terms in the expansion of the exponentials in Eq. (2) for $u(x)$ are retained. The application of the

modified boundary conditions leads to tedious formulas connecting the various amplitudes of the polariton fields. In these, linear combinations of the amplitudes emerge which are coefficients of $e^{i(k_{1x}x-\omega t)}$, in one case and those of $e^{i[(k_{1x}\pm Q)x-\omega t]}$, in the other. The coefficients of $e^{i(k_{1x}x-\omega t)}$ are associated with the specularly reflected intensity while those of the factor $e^{i(q_{1x}^{\pm}x-\omega t)}$ are associated with the diffuse reflectivities.

3. The systems studied

The formalism developed in the previous section is now applied to the two systems mentioned earlier, when the grating is on the base of the prism or on the semi-infinite specimen. The numerical values of the parameters used are as follows: $\varepsilon_1 = 11.70$, $\varepsilon_2 = 1.00$ and $\omega_T d/c = 1.15$. The values of the constants for the evaluation of the frequency-dependent dielectric function given by Eq. (1) are [1] $\varepsilon(\infty) = 9.09$, $S = 2.01$ and $\omega_T = 366\ \mathrm{cm}^{-1}$. The room-temperature value of the damping parameter, reduced by an order of magnitude, is $\Gamma/\omega_T = 5 \times 10^{-4}$. Unless otherwise stated, the grating is characterized by the amplitude and the period such that $\omega_T u_0/c = 0.05$ and $cQ/\omega_T = 0.40$, respectively.

3.1. Smooth surfaces

As mentioned earlier, if the polariton fields are expanded only up to first-order in the grating height, u_0, the equations that determine the zero-order amplitudes of the polariton fields stand alone. The specularly reflected intensity, quoted here for the sake of completeness, is found from the well-known result for the zeroth-order reflected amplitude [2,3,21]:

$$\frac{B_1}{A_1} = [\imath\varepsilon_1 a_2\beta_1 - \varepsilon_2 a_1\beta_2][\imath\varepsilon_1 a_2\beta_1 + \varepsilon_2 a_1\beta_2]^{-1}, \quad (10)$$

where

$$\beta_1 = [\varepsilon_3 a_2 \sinh(a_2 d) + \varepsilon_2 a_3 \cosh(a_2 d)], \quad (11)$$

$$\beta_2 = [\varepsilon_3 a_2 \cosh(a_2 d) + \varepsilon_2 a_3 \sinh(a_2 d)], \quad (12)$$

$$\beta_3 = [\varepsilon_3 q_{2z} \sinh(q_{2z} d) + \varepsilon_2 q_{3z} \cosh(q_{2z} d)] \quad (13)$$

and

$$\beta_4 = [\varepsilon_3 q_{2z} \cosh(q_{2z} d) + \varepsilon_2 q_{3z} \sinh(q_{2z} d)]. \quad (14)$$

The inadequacy of this first-order perturbation theory should be emphasized. As stated earlier, in the first-order perturbation theory the equations that determine the zero-order amplitudes stand alone. In reality; however, the energy carried by the higher-order fields is derived from the zeroth-order fields. Clearly there must be an intensity deficit in the specularly reflected beam which appears as the diffuse radiation. From a theoretical point of view, the amplitudes of all orders should therefore be connected in some way. The zero-order fields and both types of the first-order fields are all indeed coupled if the polariton fields are expanded at least up to the second-order in the grating amplitude. It is clear that retaining higher-order terms in the expansion of $u(x)$ necessitates incorporating higher-order polariton fields in the theoretical treatment of this problem. This more realistic approach, which only, nonetheless, adds computational complexity, is beyond the scope of this rather illustrative analysis and is therefore not persued further.

3.2. Grating on the base of the prism

The application of the modified boundary conditions leads to the following equations for the determination of the amplitudes of the first-order fields:

$$-\imath a_1(1 + k_{1x}Q/a_1^2)u_0[A_1 - B_1] + \mathscr{B}_1 = a_2(1 - k_{1x}Q/a_2^2)u_0[A_2 - B_2] + \mathscr{A}_2 + \mathscr{B}_2, \quad (15)$$

$$\varepsilon_1 q_{1z} q_{2z} u_0[A_1 + B_1] - \imath\varepsilon_1 q_{2z}\mathscr{B}_1 = \varepsilon_2 q_{1z} q_{2z} u_0[A_2 + B_2] + \varepsilon_2 q_{1z}[\mathscr{A}_2 - \mathscr{B}_2], \quad (16)$$

$$\mathscr{A}_3 e^{-q_{3z}d} = \mathscr{A}_2 e^{-q_{2z}d} + \mathscr{B}_2 e^{q_{2z}d} \quad (17)$$

and

$$\varepsilon_3 q_{2z}\mathscr{A}_3 e^{-q_{3z}d} = \varepsilon_2 q_{3z}[\mathscr{A}_2 e^{-q_{2z}d} - \mathscr{B}_2 e^{q_{2z}d}]. \quad (18)$$

The diffuse reflectivity, $\mathscr{R} = |\mathscr{B}_1/A_1|^2$, is calculated from the corresponding amplitude given by

$$\frac{\mathscr{B}_1}{A_1} = \frac{N_P}{D_P}, \tag{19}$$

where

$$N_P = 2\imath(\varepsilon_1 - \varepsilon_2)[\varepsilon_2 k_{1x} q_{1x} \beta_2 \beta_4 + \varepsilon_1 q_{2z} a_2 \beta_1 \beta_3] q_{1z} u_0 \tag{20}$$

and

$$D_P = [\imath\varepsilon_1 a_2 \beta_1 + \varepsilon_2 a_1 \beta_2][\imath\varepsilon_1 q_{2z} \beta_3 + \varepsilon_2 q_{1z} \beta_4]. \tag{21}$$

Note that for a grating of small height, the emergence of the two first-order beams is equiangular about the specularly reflected beam, at an angle ϕ such that

$$\phi = \theta \pm \tan^{-1}(q_{1x}^{\pm}/q_{1z}^{\pm}). \tag{22}$$

Fig. 1 shows the dispersion curve of surface polaritons for a semi-infinite medium, as a plot of ω/ω_T versus ck_{1x}/ω_T. The straight lines are the ATR-grating scan lines, in the frequency scan. The solid line is that associated with smooth surfaces, ck_{1x}/ω_T. The other lines are for propagation in $c(k_{1x} - Q)/\omega_T$, the dashed curve, and that for propagation in $c(k_{1x} + Q)/\omega_T$, depicted as the dotted line. Note that the dispersion curve is drawn only within the surface polariton frequency range, $\omega_T \leqslant \omega \leqslant \omega_s$, with the origin being shifted to the TO phonon frequency. The surface polariton cut-off frequency is given by [1]

$$\omega_s^2 = [(\varepsilon(\infty) + \varepsilon_2 + S)/(\varepsilon(\infty) + \varepsilon_2)]\omega_T^2. \tag{23}$$

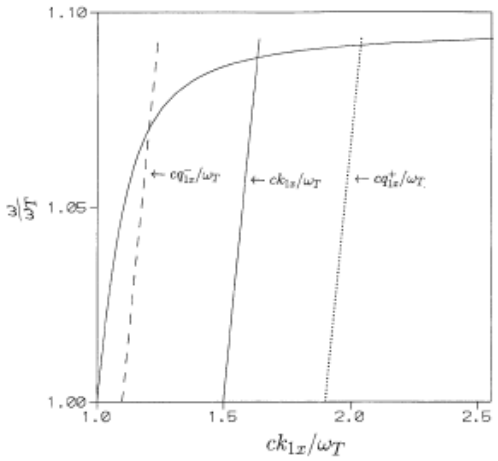

Fig. 1. The surface polariton dispersion curve for a semi-infinite planar medium. The straight lines are the typical ATR-grating coupling frequency scan lines as follows: The solid scan line corresponds to the zero-order reflectivity, that is, for propagation in k_{1x}. The dashed scan line corresponds to the first-order propagation in $k_{1x} - Q$ and the dotted line is for propagation in $k_{1x} + Q$. The angle of incidence is $\theta = 26°$.

Fig. 2a shows the diffuse reflectivities in the frequency scan for propagation in $e^{\imath(q_{1x}x - \omega t)}$ for the system when a grating of height $\omega_T u_0/c = 0.05$ and period $cQ/\omega_T = 0.40$ is deposited on the base of the prism. The different angles of incidence used to identify the individual curves are $\theta = 26°$, for the thick curve with asterisks, $\theta = 28°$, for the smooth solid curve and, $\theta = 30°$, for the dashed curve. It is seen that each curve is characterized by two polariton structures, which in this particular case are dips. These structures occur at frequencies when the tangential wave vectors of the polariton and the incoming radiation are matched at the same value of the frequency. Under these conditions, the polariton becomes radiative and, consequently, removes energy from the incident radiation. Now, recall that in the first-order perturbation theory as here, the amplitudes of the zero-order fields are coupled to the amplitudes of the first-order fields only in one of the two propagation wave numbers, $q_{1x}^- = k_{1x} - Q$ or $q_{1x}^+ = k_{1x} + Q$. In terms of the kinematics of Fig. 1, therefore, these first-order reflectivities are associated with only two scan lines, those for k_{1x} and q_{1x}^-. It is noted that the polariton structure associated with the q_{1x}^- scan line is rather broad. This is related to the nature of the surface polariton dispersion curve shown in Fig. 1. At the low frequency end, the dispersion curve is photon-like: hence, it runs almost parallel and rather close to the q_{1x}^- scan line. The damping parameter Γ actually broadens the cross-over point of the dispersion curve and the scan line. This means, at least in principle, that the polariton can still be radiative over a relatively wide range of frequency values.

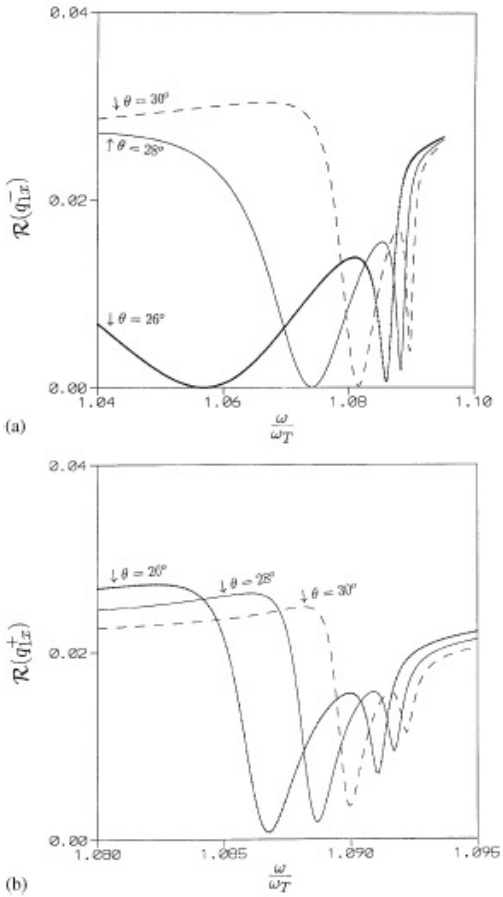

Fig. 2. (a) The diffuse reflectivities for propagation in $k_{1x} - Q$ for angles $\theta = 26°, 28°$ and $30°$ as indicated here. The grating, characterized by the period, $cQ/\omega_T = 0.4$ and the height, $\omega_T u_0/c = 0.05$ is deposited on the base of the prism. The other parameters also given in the text are $\varepsilon_1 = 11.70$, $\varepsilon_2 = 1.00$, $\varepsilon(\infty) = 9.09, s = 2.01$, $\omega_T d/c = 1.15$ and $\omega_T = 366.00\ \mathrm{cm}^{-1}$; (b) same as for (a), but for propagation in $k_{1x} + Q$.

Fig. 2b shows the frequency dependence of the first-order reflectivities for propagation in q_{1x}^+ and for exactly the same relevant parameters as for Fig. 2a. In this case, therefore, the mode is probed according to the scan lines for propagation in k_{1x} and q_{1x}^+. The two ATR dips occur more or less at the same frequency. This is hardly surprising because at the high frequency of the surface polariton spectrum, the dispersion curve is almost flat; see Fig. 1. Further, for room-temperature values of Γ, typically $5.0 \times 10^{-3}\omega_T$, the two dips merge into one relatively broad dip and therefore are not resolved. One implication of this resonance broadening is that the presence of a grating on the base of the prism enhances the absorption of energy by the polariton from the incident radiation. As anticipated, the polariton structures shift to higher frequencies as the angle of incidence is increased. An increase of the angle of incidence results in the increase of the tangential wave vector of the incoming radiation. Consequently, the polariton becomes radiative at higher frequencies, or at larger tangential wave vectors of the polariton. In terms of the kinematics of Fig. 1, an increase in θ means that the ATR-grating scan lines are displaced to the right. The scan lines therefore intersect the polariton dispersion curve at higher frequency values.

3.3. Grating on the specimen

Following exactly the same analysis as in the previous sub-section, the amplitude of the first-order reflected wave for propagation in $e^{i(q_{1x}^- x - \omega t)}$ is found to be:

$$\frac{\mathscr{B}_1}{A_1} = \frac{N_S}{D_S}, \tag{24}$$

in which

$$N_S = 2\imath\varepsilon_1\varepsilon_2(\varepsilon_2 - \varepsilon_3)[\varepsilon_3 k_{1x} q_{1x} + \varepsilon_2 a_3 q_{3z}] q_{1z} q_{2z} a_2 u_0 \tag{25}$$

and

$$D_s = D_P. \tag{26}$$

The first-order diffuse reflectivities for this system, when the grating is inscribed on the surface-active medium, are shown in Fig. 3. Note that these reflectivities have been amplified by a factor of a thousand as they are much weaker compared to those for the system in which the grating is on the base of the prism. Fig. 3a is for propagation in q_{1x}^- and Fig. 3b is for propagation in the other (q_{1x}^+) first-order wave number. The relevant parameters

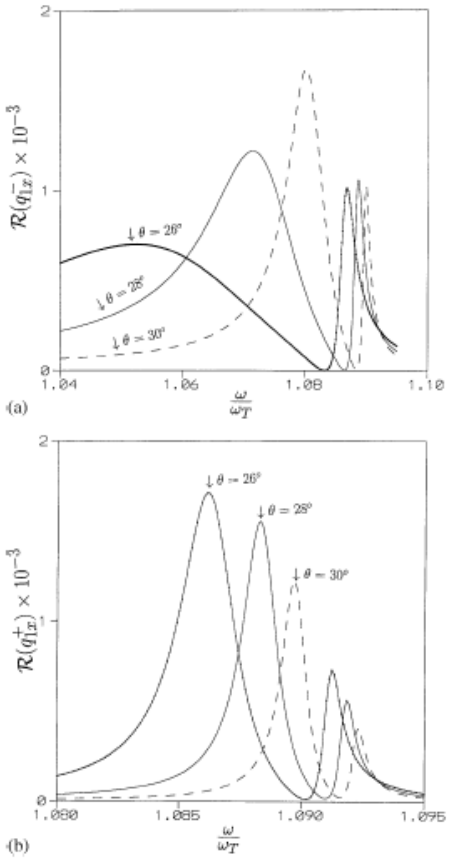

Fig. 3. (a) Same caption as for Fig. 2a except that here the grating is deposited on the specimen; (b) same as for (a), but for propagation in $k_{1x} + Q$.

are as for Fig. 2, in particular, $\theta = 26°$, for the thick curve with asterisks, $\theta = 28°$, for the smooth solid curve and $\theta = 30°$ for the dashed curve. As in the previous section, the frequency positions of the polariton structures can be predicted following the simple kinematics of Fig. 1. The immediate observation regarding the reflectivities depicted in Fig. 3 is that the polariton structures are peaks. This is in stark contrast to the case when the grating is on the base of the prism. It is noted that when the grating is inscribed on a semi-infinite medium, upon becoming radiative, the surface polariton can in fact emit energy [9]. This has also been confirmed in the recent investigations in which plasmon polaritons were probed using an array of holes [15]. It is also noted that when the grating is on the specimen, the frequency positions of the polariton structures show a pronounced departure from predictions based on the kinematics of Fig. 1. This is viewed as an indication that the presence of roughness on a surface-active medium, even if periodically deterministic, does indeed perturb the mode under investigation.

The combined technique of ATR-grating coupling potentially has substantial advantages over the constituent methods when each is employed on its own. To start with, in ATR alone the smallest angle of incidence is the prism-air critical angle. This means that in ATR alone the section of the surface polariton dispersion curve to the left of the scan line corresponding to θ_c, namely, $ck_{1x}/\omega_T = \sqrt{\varepsilon_1}(\omega/\omega_T)\sin\theta_c$, can never be accessed. On the other hand, in grating coupling alone, the $c(k_{1x} - Q)/\omega_T$ scan lines do not intersect the non-radiative branch of the surface polariton curve. In as far as exhibiting the degree of dispersion, this is the most interesting section of the surface polariton curve; however, it is inaccessible in either of the constituent methods when each is employed alone. Further, being associated with the highest number of scan lines, ATR-grating coupling is bound to be the most efficient of the three methods for measuring dispersion curves. At least from the theoretical point of view, it appears that in ATR-grating coupling the higher-order reflectivities can easily be of the same order of magnitude as the specular intensity. It should also be pointed out that, at least in principle, it is not necessary to produce several gratings of different periods as was done by Wendler et al. [14]. The one grating of small period can be rotated through an angle γ about the normal to the interfaces. In that case, the surface then presents an effective reciprocal lattice vector, $Q_{\text{eff}} = Q/\cos\gamma$, with the result that the whole of the surface polariton dispersion curve can be spanned. In this way, at least in principle, covering the whole dispersion curve can be achieved even for only one angle of incidence.

From an experimental point of view, the preferred configuration should be the one when the grating is on the base of the prism rather than on the specimen. Apart from permanently disfiguring the sample by inscribing a grating on it, the very mode under investigation will be perturbed by surface roughness. There is also the possibility of altering the optical properties of the surface-active medium. This will introduce yet another difficulty in the interpretation of the results or, more to the point, reconciling experiment with theory. The complication of having to select parameters for the characterization of the grating that give optimum coupling can also be avoided by having a grating on the base of the prism. As is evident in the investigations by Wendler et al. [14], the polariton structures in the transmission spectra can be maxima or minima, in a rather less predictable way, depending on the parameters for the characterization of surface roughness. In fact, it was found that for some parameters of the grating, the polariton structures were barely discernible.

4. Concluding remarks

The experimental technique of grating coupling as a probe for surface excitations was revised but in combination with the method of attenuated total reflection. The ATR set-up in the Otto [18] was considered and, in addition, a classical grating was assumed to be deposited on only one of the interfaces. The main results of these investigations were the first-order diffuse reflectivities. These were obtained within first-order perturbation theory, taking the grating as a perturbation from the otherwise assumed planar character of the interfaces. The two systems considered were when the grating is either on the base of the prism or when it is on a semi-infinite specimen. It was found that when the grating is on the base of the prism the diffuse reflectivities are characterized by minima. The minima occur at frequencies when the tangential components of polariton and incident radiation, at a particular frequency, are matched. This signifies the absorption of a part of the incident energy by the polariton from the incoming radiation. In the case where the grating is on the specimen, however, the polariton structures are peaks. For this system, therefore, on becoming radiative, the polariton emits energy. This is the energy associated with the momentum $\hbar Q$ imparted to the polariton by the crystal due to surface roughness. It is noted that even for a grating of small height, the E_n component of electric field oscillates about the normal to the undulation. The polariton consequently radiates energy more or less like an oscillating electric dipole. The combined method of ATR-grating coupling arguably has some advantages over each of the constituent probes for polaritons. In the combined technique, it becomes possible to access the section of the polariton dispersion curve to the left of the ATR scan-lines associated with incident angles that are less than the critical angle. The combined technique is the most efficient in so far as spanning the whole of the dispersion curve. This is because ATR-grating coupling is associated with the highest number of scan lines which essentially cover the whole surface polariton dispersion curve. In any case, probing any section of the dispersion curve can also be achieved by appropriately rotating the grating thereby varying the effective period of the grating. From an experimental point of view, the preferred configuration would be when the grating is inscribed on the base of the prism rather than on the surface-active medium. Imprinting a grating on the specimen can result in permanent disfigurement and possibly the alteration of the optical properties of the sample. Perhaps it is more important that the very mode under investigation will be perturbed by surface roughness on the specimen. This is possible even for small values of u_0 since surface modes can be very strongly localized at the interface.

Finally, for a future outlook, the analysis carried out here may be extended to the more realistic systems, such as those studied by Heitmann and Raether [13], of thin film samples. The polariton fields, on application of the boundary conditions, could be expanded to at least the second-order in the grating amplitude. In this way, the influence of the grating on the specularly reflected intensity could be evaluated.

References

[1] J.S. Nkoma, D.R. Tilley, R. Loudon, J. Phys. C 7 (1974) 3547.
[2] M.G. Cottam, D.R. Tilley, Introduction to Surface and Superlattice Excitations, Cambridge University Press, Cambridge, 1989.
[3] V.M. Agranovich, D.L. Mills, Surface polaritons, North-Holland, Amsterdam, 1982.
[4] J.S. Nkoma, Solid State Commun. 87 (1993) 241.
[5] T. Kume, S. Hayashi, K. Yamamoto, Phys. Rev. B 55 (1997) 4774.
[6] B. Fischer, N. Marschall, H. Queisser, Phys. Rev. Lett. 27 (1971) 95.
[7] M.C. Hutley, Diffraction Gratings, Academic Press, London, 1982.
[8] V.M. Agranovich, R. Loudon, Surface Excitations, North-Holland, Amsterdam, 1984.
[9] H. Raether, Surface Plasmons on Smooth and Rough Surfaces and on Gratings, Springer, Berlin, 1988.
[10] A.A. Maradudin, A. Marvin, M. Haller, V. Celli, G. Brown, Phys. Rev. B 31 (1985) 4993.
[11] A.A. Maradudin, B. Laks, D.L. Mills, Phys. Rev. B 23 (1981) 4863.
[12] I. Pockrand, Phys. Lett. 49A (1974) 259.
[13] D. Heitmann, H. Raether, Surf. Sci. 59 (1976) 17.
[14] L. Wendler, T. Kraft, M. Hartung, A. Berger, A. Wixforth, M. Sundram, J.H. English, A.C. Gossard, Phys. Rev. B 55 (1997) 2303.
[15] T.W. Ebbesen, H.J. Lezec, H.F. Ghaemi, T. Thio, P.A. Wolff, Nature 391 (1998) 667.
[16] L. Salomon, F. Grillot, A.V. Zayats, F. de Fornel, Phys. Rev. Lett. 86 (2001) 1110.
[17] L. Martín-Moreno, F.J. García-Vidal, H.J. Lezec, K.M. Pellerin, T. Thio, J.B. Pendry, T.W. Ebbesen, Phys. Rev. Lett. 86 (2001) 1114.
[18] A. Otto, Z. Phys. 216 (1968) 398.
[19] A. Marvin, V. Celli, F. Toigo, Phys. Rev. B 11 (1975) 706.
[20] A. Marvin, V. Celli, R. Hill, F. Toigo, Phys. Rev. B 15 (1977) 5618.
[21] V.V. Bryksin, Yu.M. Gerbstein, D.N. Mirlin, Sov. Phys.-Solid State 14 (1972) 453.